CMI

ARTICLE

Check for updates

RIPK1 plays a crucial role in maintaining regulatory T-Cell homeostasis by inhibiting both RIPK3- and FADD-mediated cell death

Xiaoxue Deng[1,2,6], Lingxia Wang[3,6], Yunze Zhai[1,2,6], Qiuyue Liu[1], Fengxue Du[1], Yu Zhang[2], Wenxing Zhao[2], Tingtao Wu[2], Yiwen Tao[4], Jie Deng[5], Yongbing Cao[5], Pei Hao[2], Jiazi Ren[1], Yunli Shen[1], Zuoren Yu[1], Yuejuan Zheng[4]✉, Haibing Zhang[3]✉ and Haikun Wang[1,2]✉

Regulatory T (T_{reg}) cells play an essential role in maintaining immune balance across various physiological and pathological conditions. However, the mechanisms underlying T_{reg} homeostasis remain incompletely understood. Here, we report that RIPK1 is crucial for T_{reg} cell survival and homeostasis. We generated mice with T_{reg} cell-specific ablation of *Ripk1* and found that these mice developed fatal systemic autoimmunity due to a dramatic reduction in the T_{reg} cell compartment caused by excessive cell death. Unlike conventional T cells, T_{reg} cells with *Ripk1* deficiency were only partially rescued from cell death by blocking FADD-dependent apoptosis. However, simultaneous removal of both *Fadd* and *Ripk3* completely restored the homeostasis of *Ripk1*-deficient T_{reg} cells by blocking two cell death pathways. Thus, our study highlights the critical role of RIPK1 in regulating T_{reg} cell homeostasis by controlling both apoptosis and necroptosis, thereby providing novel insights into the mechanisms of T_{reg} cell homeostasis.

Keywords: T_{reg} cell; Homeostasis; Apoptosis; Necroptosis

Cellular & Molecular Immunology (2024) 21:80–90; https://doi.org/10.1038/s41423-023-01113-x

INTRODUCTION

Regulatory T (T_{reg}) cells, a subset of $CD4^+$ T cells, are essential for maintaining immune homeostasis and self-tolerance [1]. While T_{reg} cells are mainly generated in the thymus, they can also be induced from naive T cells in the periphery. In the steady state, T_{reg} cells are a relatively stable population, and abnormalities in their homeostasis are often associated with autoimmune or immunodeficient diseases. To maintain this relative stability, T_{reg} cells need to coordinate survival and death signals from cytokines, TCR/costimulatory signaling and anatomical location [2]. Similar to the role of IL-7 in conventional T-cell homeostasis, IL-2 plays a pivotal role in promoting T_{reg} cell homeostasis by driving the upregulation of antiapoptotic proteins [3, 4]. However, not all T_{reg} cells depend on IL-2 for homeostatic maintenance. For example, $CD62L^{low}CD44^{high}$ activated T_{reg} (aT_{reg}) cells rely on TCR signals and the costimulatory molecule ICOS to maintain their phenotypical identity and homeostasis [5, 6]. Sensing and responding to diverse survival or death signals, many intracellular factors are also involved in the maintenance of T_{reg} population homeostasis. Some studies have shown that Bak- and Bax-mediated intrinsic apoptosis pathways help constrain the T_{reg} population, but Mcl-1, upregulated by IL-2 signals, inhibits Bak- and Bax-mediated T_{reg} cell apoptosis [3]. Compared to extrinsic signals, the intracellular factors that regulate T_{reg} homeostasis remain poorly understood.

Receptor-interacting protein kinase 1 (RIPK1) plays a vital role in regulating apoptosis, necroptosis and inflammation, depending on the cellular context. Among these pathways, the TNFR1-mediated RIPK1 activation pathway has been extensively studied. Upon activation by TNF-α, TNFR1 recruits TNFR-associated death domain protein (TRADD), RIPK1, TRAF2, and cIAP1/2 to form complex I [7]. Within complex I, RIPK1 undergoes polyubiquitination, activating the pro-survival NF-kappa B (NF-κB) pathway. If complex I is disturbed, a new cytosolic complex IIa is formed by internalized TNFR1 and deubiquitinated RIPK1, resulting in cell apoptosis [8, 9]. In cases where apoptosis is inhibited, RIPK1 interacts with RIPK3 through the RIP homotypic interaction motif (RHIM) to form complex IIb, which facilitates the phosphorylation and oligomerization of mixed lineage kinase domain-like protein

[1]State Key Laboratory of Cardiology, Shanghai East Hospital, Tongji University School of Medicine, Shanghai 200120, China. [2]CAS Key Laboratory of Molecular Virology and Immunology, Shanghai Institute of Immunity and Infection, Chinese Academy of Sciences, University of Chinese Academy of Sciences, Shanghai 200031, China. [3]CAS Key Laboratory of Nutrition, Metabolism and Food Safety, Shanghai Institute of Nutrition and Health, Shanghai Institutes for Biological Sciences, University of Chinese Academy of Sciences, Chinese Academy of Sciences, Shanghai 200031, China. [4]The Research Center for Traditional Chinese Medicine, Shanghai Institute of Infectious Diseases and Biosecurity, Shanghai University of Traditional Chinese Medicine, Shanghai 201203, China. [5]Institute of Vascular Disease, Shanghai TCM-Integrated Hospital, Shanghai University of Traditional Chinese Medicine, Shanghai 200433, China. [6]These authors contributed equally: Xiaoxue Deng, Lingxia Wang, Yunze Zhai. ✉email: 13641776412@163.com; hbzhang@sibs.ac.cn; 15001995464@163.com

Received: 16 July 2023 Accepted: 13 November 2023
Published online: 11 December 2023

(MLKL), resulting in necroptosis [10, 11]. Consistent with these findings, genetic studies in mice have demonstrated the crucial role of RIPK1 in maintaining tissue homeostasis by regulating apoptosis, necroptosis, and inflammation. Specifically, *Ripk1*-deficient mice die at birth due to systemic inflammation, which can be prevented by inhibiting both FADD/Caspase8-dependent apoptosis and RIPK3/MLKL-dependent necroptosis [12]. Furthermore, studies on conditional *Ripk1* knockout mice have shown that RIPK1 plays a critical role in regulating skin and intestinal inflammation, autoimmunity, and tissue fibrosis [13–15].

In addition, recent studies have identified individuals with biallelic loss-of-function mutations in the RIPK1 gene who displayed a range of clinical manifestations with lymphopenia [16, 17]. Consistently, mice with targeted deletion of RIPK1 in T cells also showed severe T lymphopenia [18]. These findings strongly indicate the importance of RIPK1 in T-cell function and highlight its relevance in the immune system. However, considering that T_{reg} cells have unique homeostatic mechanisms distinct from those found in conventional T cells, there is still great interest in investigating whether RIPK1 plays a role in T_{reg} cell homeostasis and function. In this study, we generated mice with specific *Ripk1* ablation in T_{reg} cells and found that these mice developed fatal systemic autoimmunity due to a significant reduction in the T_{reg} cell compartment caused by excessive cell death. Unlike conventional T cells, which undergo FADD-dependent apoptosis when RIPK1 is absent, T_{reg} cells with *Ripk1* deficiency exhibit only partial rescue with *Fadd* deletion. Rather, we discovered that simultaneous inhibition of both FADD-dependent apoptosis and RIPK3-dependent necroptosis fully rescued *Ripk1*-deficient T_{reg} cells from excessive death. These results highlight the critical role of RIPK1 in regulating T_{reg} cell survival by controlling both apoptosis and necroptosis, providing new insights into the mechanisms underlying T_{reg} cell homeostasis.

RESULTS

RIPK1 is upregulated in activated T_{reg} cells

To gain a better understanding of the role of RIPK1 in T_{reg} cells, we first examined its expression in these cells. Based on the expression levels of the cell surface markers CD44 and CD62L, T_{reg} cells can be divided into two populations: a resting T_{reg} cell population (rT_{reg}) characterized by $CD44^{low}CD62L^{high}$ and an activated T_{reg} cell population (aT_{reg}) characterized by $CD44^{high}CD62L^{low}$ [19, 20]. Both immunoblotting and intracellular staining results revealed that aT_{reg} cells expressed higher levels of RIPK1 than quiescent rT_{reg} cells (Fig. 1A, B). Interestingly, effector T_{reg} cells, identified as $KLRG1^+ICOS^+$ aT_{reg} cells, exhibited the highest level of RIPK1 among all T_{reg} cells (Fig. 1B). TCR signals are important for the phenotypical identity of aT_{reg} cells [5]. The high expression of RIPK1 in aT_{reg} cells led us to suspect that it may be regulated by TCR signals. We observed that TCR stimulation in vitro for 24 h significantly increased the protein level of RIPK1 in T_{reg} cells (Fig. 1C). Notably, IL-2 stimulation did not lead to an upregulation of RIPK1 expression in T_{reg} cells (Supplementary Fig. 1A). These results suggest that RIPK1 is differentially expressed in T_{reg} cells under different activation states and may have varying roles in different populations of T_{reg} cells.

T_{reg} cell-specific ablation of *Ripk1* results in fatal systemic autoimmunity

To investigate the role of RIPK1 in T_{reg} cells, we crossed mice with loxP-flanked *Ripk1* alleles ($Ripk1^{f/f}$) with $Foxp3^{YFP\text{-}Cre}$ knock-in mice ($Foxp3^{Cre}$) to delete RIPK1 specifically in T_{reg} cells ($Ripk1^{f/f}Foxp3^{Cre}$) (Supplementary Fig. 1B). The $Ripk1^{f/f}Foxp3^{Cre}$ mice showed stunted growth and a markedly reduced lifespan, typically surviving only 3–12 weeks (Fig. 1D, E). These mice also manifested significant splenomegaly and lymphadenopathy (Fig. 1D). Histological analysis revealed extensive leukocyte infiltration in the skin, lung, liver, and colon of $Ripk1^{f/f}Foxp3^{Cre}$ mice (Fig. 1F). Flow cytometry analysis consistently showed a substantially higher percentage of $Gr\text{-}1^+$ myeloid cells in the lymph nodes of these mice (Supplementary Fig. 1C). Furthermore, there was a significant increase in $CD44^{high}CD62L^{high}$ memory or $CD44^{high}CD62L^{low}$ effector T cells in these mice, which produced increased levels of effector cytokines such as IFN-γ, IL-4 and IL-17A in $CD4^+$ T cells, as well as IFN-γ and granzyme B in $CD8^+$ T cells (Fig. 1G, H, Supplementary Fig. 1D). These phenotypes indicate severe defects in T_{reg} cells resulting from *Ripk1* deletion.

RIPK1 is crucial for maintaining peripheral T_{reg} cell homeostasis

We proceeded to analyze the frequencies of T_{reg} cells in the thymus, as well as various lymphoid and nonlymphoid organs, in both $Ripk1^{f/f}Foxp3^{Cre}$ mice and control $Foxp3^{Cre}$ mice aged 2 to 6 weeks. Our findings revealed a significant reduction in the percentages of T_{reg} cells in the spleens, lymph nodes, lungs, livers, small intestines and colons of $Ripk1^{f/f}Foxp3^{Cre}$ mice (Fig. 2A, B). Interestingly, these decreases in T_{reg} cell percentages were already observed in $Ripk1^{f/f}Foxp3^{Cre}$ mice as early as 3 weeks of age (Fig. 2A, B). It is worth noting that these reductions in T_{reg} cells were not attributed to developmental defects since the frequencies of T_{reg} cells in the thymi of wild-type mice were comparable to those in the thymi of $Ripk1^{f/f}Foxp3^{Cre}$ or $Ripk1^{f/f}CD4^{Cre}$ mice (Fig. 2A, B, Supplementary Fig. 2A, B). These results strongly suggest that RIPK1 serves as a crucial regulator of T_{reg} cell homeostasis in the periphery.

To investigate whether RIPK1 intrinsically regulates T_{reg} cell homeostasis, we analyzed T_{reg} cells in female $Ripk1^{f/f}Foxp3^{Cre/+}$ and $Foxp3^{Cre/+}$ mice. In female $Ripk1^{f/f}Foxp3^{Cre/+}$ mice, a portion of T_{reg} cells retained RIPK1 due to random X-chromosome inactivation, which prevented the development of autoimmune diseases. Our analysis revealed a gradual decrease in RIPK1-deficient YFP^+ T_{reg} cells starting at 4 weeks of age in female $Ripk1^{f/f}Foxp3^{Cre/+}$ mice compared to their counterparts in female $Foxp3^{Cre/+}$ mice (Fig. 2C). Interestingly, the loss of $CD44^{high}CD62L^{low}$ aT_{reg} cells was more pronounced in female $Ripk1^{f/f}Foxp3^{Cre/+}$ mice than the loss of $CD44^{low}CD62L^{high}$ rT_{reg} cells (Fig. 2D), which aligns with the higher RIPK1 protein expression in aT_{reg} cells. Thus, our findings suggest that RIPK1 plays a crucial role in regulating T_{reg} cell homeostasis in the periphery through an intrinsic cellular mechanism.

T_{reg} cells lacking RIPK1 are more susceptible to cell death

RIPK1 plays a dual role in regulating cell survival and death under different conditions. To investigate the primary cause of T_{reg} cell reduction in $Ripk1^{f/f}Foxp3^{Cre}$ mice, we first examined cell death in T_{reg} cells, and we found that ex vivo RIPK1-deficient T_{reg} cells exhibited a higher rate of apoptotic cell death, as indicated by the Annexin $V^+7\text{-}AAD^-$ cell population (Fig. 3A). Similarly, both rT_{reg} and aT_{reg} cells from $Ripk1^{f/f}Foxp3^{Cre}$ mice expressed elevated levels of cleaved caspase-3 protein compared with their wild-type counterparts (Fig. 3B, Supplementary Fig. 3A), indicating that RIPK1-deficient T_{reg} cells are more susceptible to apoptosis. Although IL-2 and TCR signals are essential for T_{reg} cell homeostasis, we observed no significant differences in cell death between RIPK1-sufficient and RIPK1-deficient cells when treated with IL-2 (Fig. 3C, Supplementary Fig. 3B). This suggests that RIPK1 may not be needed for IL-2-mediated T_{reg} cell survival. However, TCR stimulation resulted in significantly increased cell death in RIPK1-deficient cells (Fig. 3C, D, Supplementary Fig. 3B), indicating that RIPK1 potentially offers crucial protection against activation-induced T_{reg} cell death. Notably, we found no obvious defects in the proliferation of RIPK1-deficient T_{reg} cells through Ki-67 protein staining and CellTrace dilution analysis (Supplementary Fig. 3C, D).

To gain further insights into the regulation of T_{reg} cell homeostasis and functions by RIPK1, we performed a

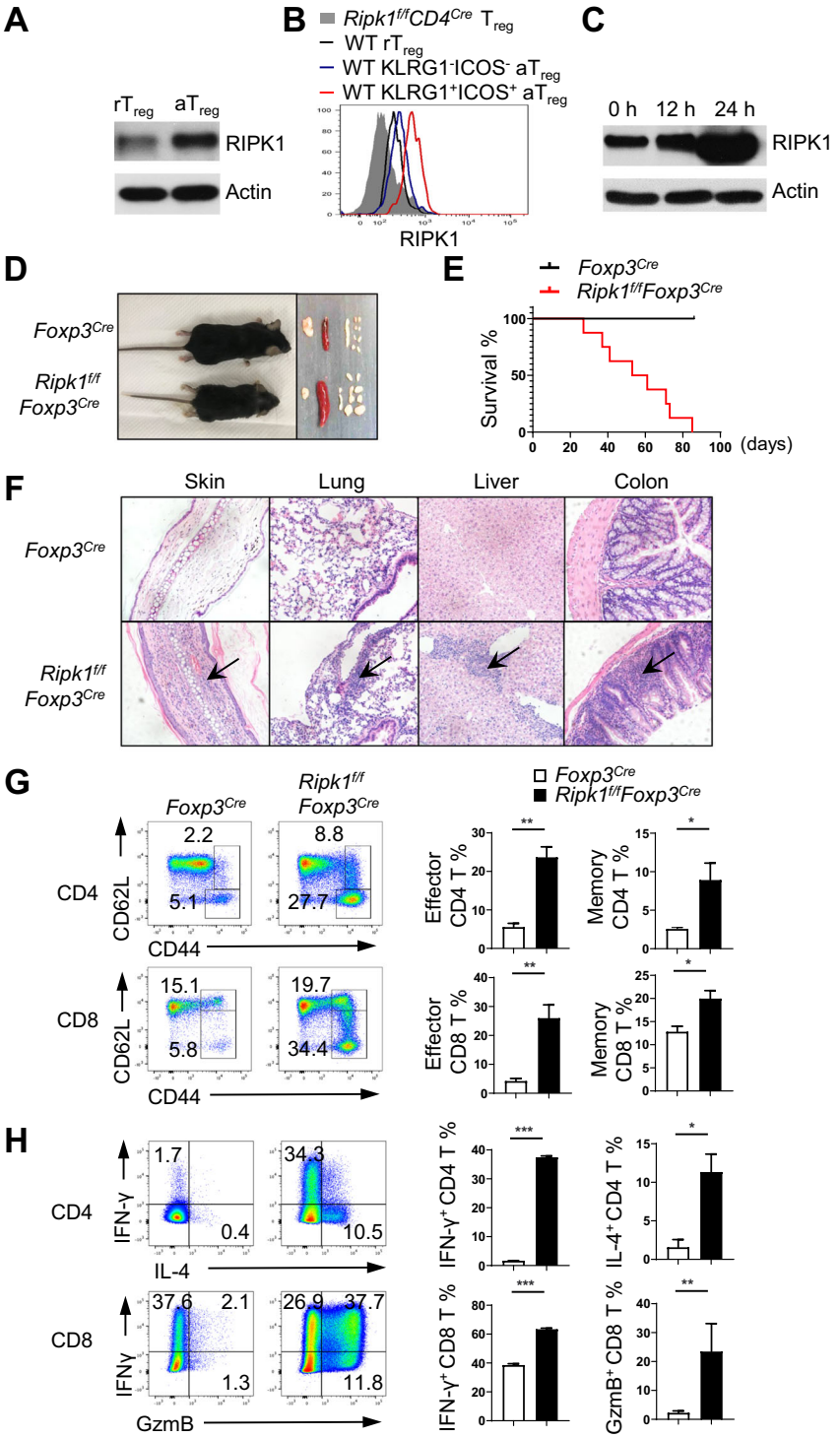

Fig. 1 T_{reg} cell-specific deletion of RIPK1 leads to fatal systemic autoimmunity. **A** Immunoblot analysis of RIPK1 expression in sorted $YFP^+CD4^+CD44^{low}CD62L^{high}$ T_{reg} cells (rT_{reg} cells) and $YFP^+CD4^+CD44^{high}CD62L^{low}$ T_{reg} cells (aT_{reg} cells) from *Foxp3*^{Cre} mice. **B** Intracellular staining of RIPK1 expression in rT_{reg} cells, $KLRG1^{low}ICOS^{low}$ aT_{reg} and $KLRG1^{high}ICOS^{high}$ aT_{reg} cells from wild-type (WT) mice and T_{reg} cells from *Ripk1*$^{f/f}$*CD4*^{Cre} mice. **C** Immunoblotting of RIPK1 in sorted YFP^+ WT T_{reg} cells stimulated with plate-bound anti-CD3/CD28 for the indicated time points. **D** Representative images of 6-week-old *Foxp3*^{Cre} and *Ripk1*$^{f/f}$*Foxp3*^{Cre} mice and the lymph organs isolated from these mice. **E** Survival curve of *Foxp3*^{Cre} and *Ripk1*$^{f/f}$*Foxp3*^{Cre} mice at the indicated time points ($n = 10$). **F** Hematoxylin and eosin staining of the indicated organs from *Foxp3*^{Cre} and *Ripk1*$^{f/f}$*Foxp3*^{Cre} mice. Arrows indicate the areas of immune cell infiltration. The magnification is 100×. **G** Flow cytometry analysis of CD44 and CD62L expression on T cells in the lymph nodes of 6-week-old *Foxp3*^{Cre} and *Ripk1*$^{f/f}$*Foxp3*^{Cre} mice. Numbers adjacent to the outlined areas indicate the percentages of $CD44^{high}CD62L^{low}$ activated T cells. **H** Flow cytometry analysis of IFN-γ and IL-4 expression in $CD4^+$ T cells and IFN-γ and granzyme B (GzmB) expression in $CD8^+$ T cells in the lymph nodes of 6-week-old *Foxp3*^{Cre} and *Ripk1*$^{f/f}$*Foxp3*^{Cre} mice after 6-h stimulation with PMA plus ionomycin. Numbers in quadrants indicate the percentage of cells in each respective quadrant. Data in (**A**–**C**) are representative of at least two independent experiments. Data in (**D**, **F**–**H**) are representative of at least three independent experiments

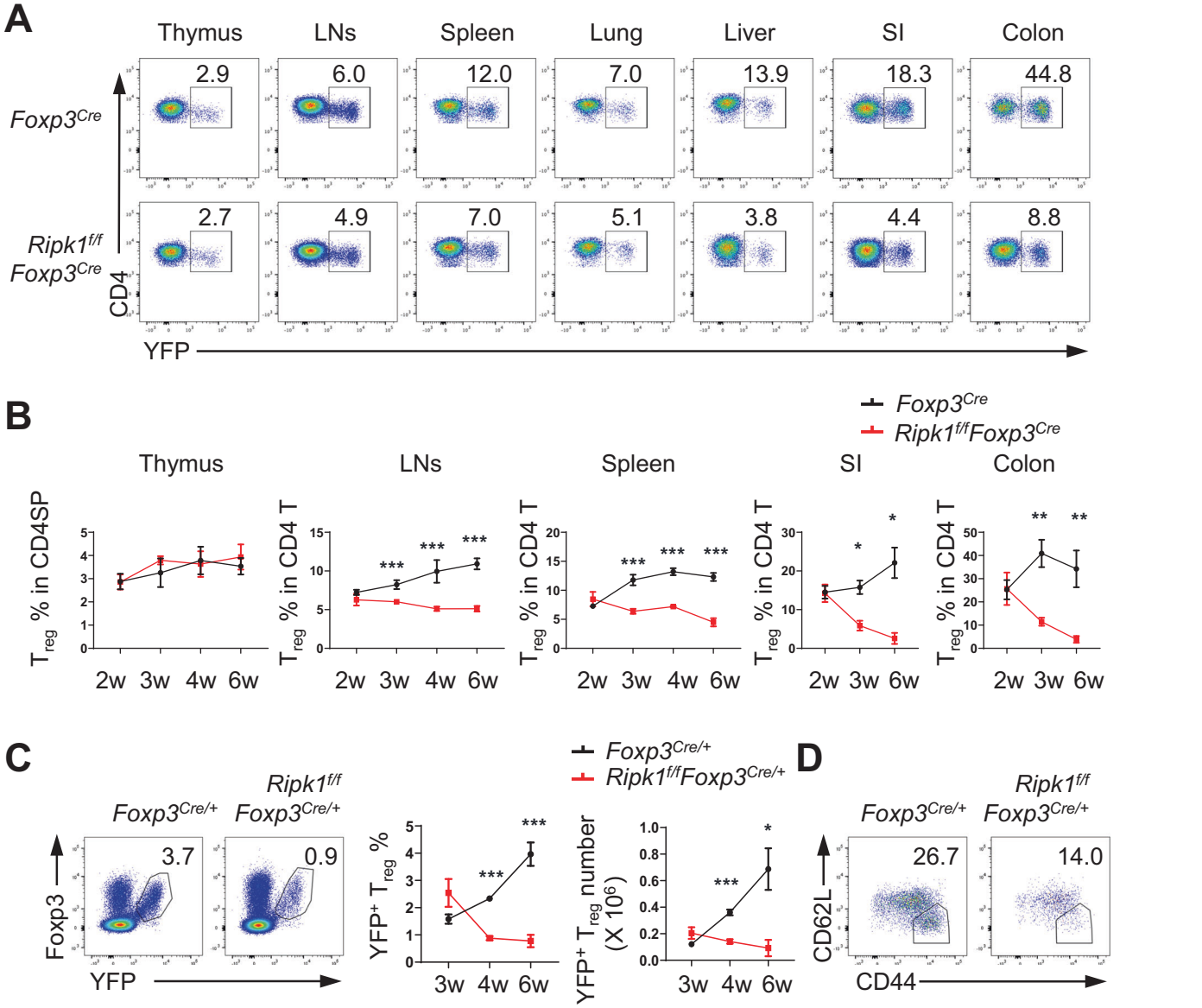

Fig. 2 RIPK1 is critical for the maintenance of peripheral T_{reg} homeostasis. **A** Flow cytometry analysis of YFP$^+$ T_{reg} cells in CD4SP thymocytes in the thymus or in CD4$^+$ T cells in the lymph nodes (LNs), spleen, lungs, liver, small intestine and colon of 3-week-old *Foxp3^{Cre}* and *Ripk1$^{f/f}$Foxp3^{Cre}* mice. Numbers adjacent to the outlined areas indicate the percentages of YFP$^+$ T_{reg} cells. **B** Kinetics of the frequencies of YFP$^+$ T_{reg} cells in the indicated organs from *Foxp3^{Cre}* and *Ripk1$^{f/f}$Foxp3^{Cre}* mice at the indicated ages ($n = 3$–5). **C** Flow cytometry analysis of YFP$^+$Foxp3$^+$ T_{reg} cells in the lymph nodes of female *Foxp3$^{Cre/+}$* and *Ripk1$^{f/f}$Foxp3$^{Cre/+}$* mice. The left panel shows a representative flow cytometry plot highlighting YFP$^+$Foxp3$^+$ T_{reg} cells in CD4$^+$ T cells in the lymph nodes of 6-week-old female *Foxp3$^{Cre/+}$* and *Ripk1$^{f/f}$Foxp3$^{Cre/+}$* mice, with numbers adjacent to the outlined areas indicating the percentages of YFP$^+$Foxp3$^+$ T_{reg} cells. The right panel summarizes the frequencies and numbers of YFP$^+$Foxp3$^+$ T_{reg} cells in the lymph nodes of female *Foxp3$^{Cre/+}$* and *Ripk1$^{f/f}$Foxp3$^{Cre/+}$* mice at the indicated ages ($n = 4$). **D** Flow cytometry analysis of CD44^{High}CD62L^{low} activated T_{reg} (aT_{reg}) cells among the YFP$^+$ T_{reg} cells in the lymph nodes of 6-week-old female *Foxp3$^{Cre/+}$* and *Ripk1$^{f/f}$Foxp3$^{Cre/+}$* mice. The numbers adjacent to the outlined areas indicate the percentages of aT_{reg} cells. Data in (**A**–**D**) are representative of at least two independent experiments. Data in (**B**, **C:** right panel) are mean ± s.e.m., ns not significant, *$p < 0.05$, **$p < 0.01$, ***$p < 0.001$ (two-tailed Student's *t* test)

comprehensive analysis of the gene expression profiles of rT_{reg} and aT_{reg} cells from *Ripk1$^{f/f}$Foxp3^{Cre}* and wild-type mice using RNA-Seq and flow cytometry analysis. Our findings showed that the expression levels of T_{reg} cell core signature genes and proteins such as *Foxp3*, *Ctla4*, *Il10* and *Tgfb1* in *Ripk1$^{f/f}$Foxp3^{Cre}* T_{reg} cells were not lower than those in wild-type T_{reg} cells (Fig. 3E, Supplementary Fig. 4A–D), indicating that the loss of RIPK1 does not disrupt T_{reg} cell development. However, we observed that *Ripk1$^{f/f}$Foxp3^{Cre}* T_{reg} cells exhibited some phenotypic and transcriptomic features of cytotoxic T cells. Specifically, the expression levels of *Tbx21*, *Cxcr3*, *Ifng*, *Gzma* and *Gzmb* were substantially higher in *Ripk1$^{f/f}$Foxp3^{Cre}* T_{reg} cells than in wild-type T_{reg} cells (Fig. 3E–G), suggesting that RIPK1 may play a critical role in maintaining T_{reg} cell identity and function. As expected, *Ripk1$^{f/f}$Foxp3^{Cre}* T_{reg} cells showed reduced expression levels of anti-apoptotic genes, such as *Bcl2* and *Bcl2l2*, while the levels of proapoptotic genes, such as *Bak1* and *Casp3*, were elevated (Fig. 3E, F). However, we found no significant changes or only slight increases in the expression levels of apoptosis-related and necroptosis-related receptors such as TNFR1, CD95, and PD-1 (Supplementary Fig. 4A, B). This suggests that RIPK1 promotes T_{reg} cell survival independent of the regulation of these cell death-

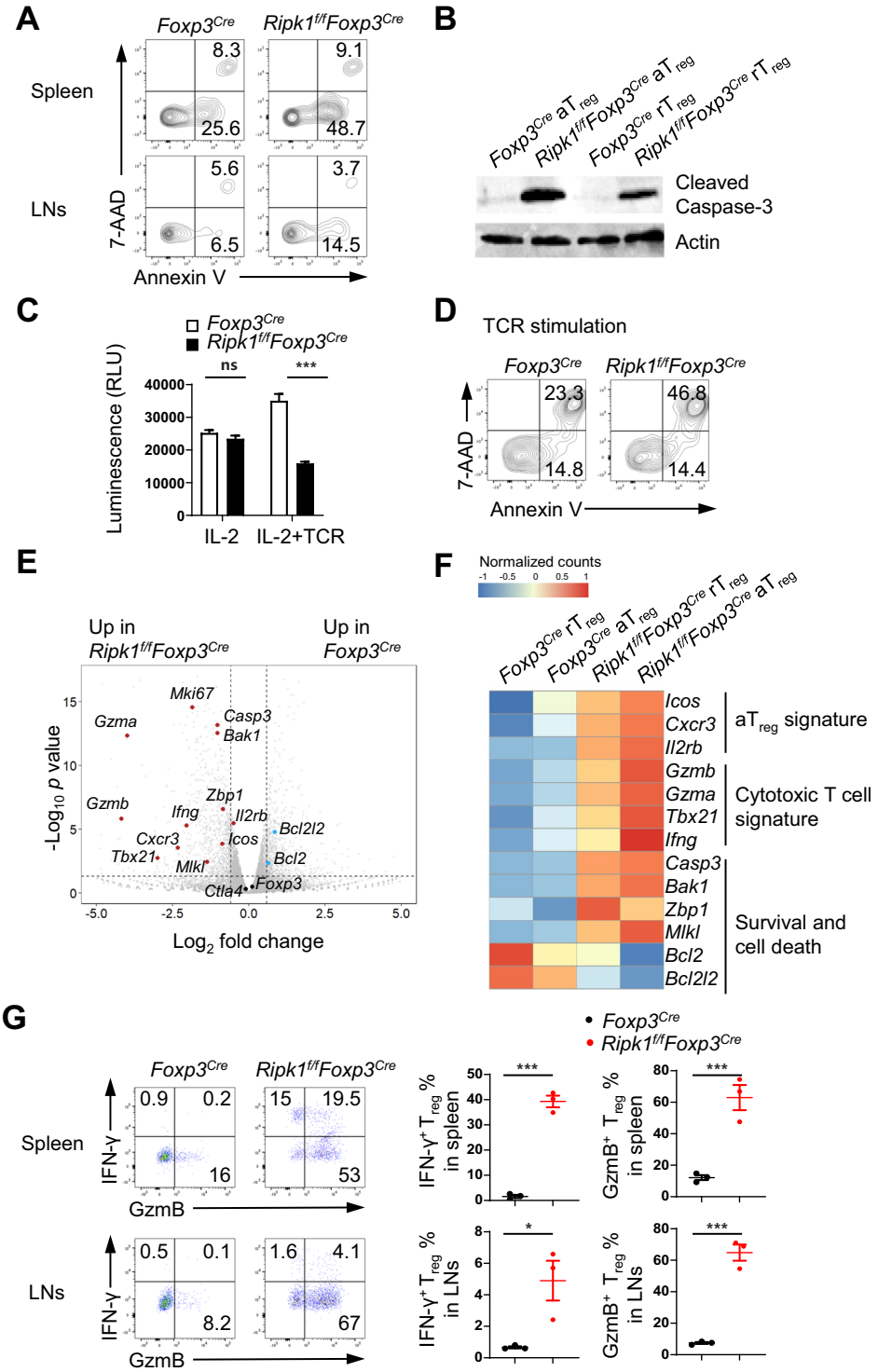

Fig. 3 RIPK1-deficient T_{reg} cells have a higher susceptibility to cell death. **A** Flow cytometry analysis of apoptotic and dead YFP$^+$ T_{reg} cells from 6-week-old *Foxp3*^{Cre} and *Ripk1*$^{f/f}$*Foxp3*^{Cre} mice using Annexin V and 7-AAD staining. **B** Immunoblotting of cleaved Caspase-3 protein in sorted aT_{reg} and rT_{reg} cells from 3-week-old *Foxp3*^{Cre} and *Ripk1*$^{f/f}$*Foxp3*^{Cre} mice. **C** Cell viability analysis of sorted T_{reg} cells from *Foxp3*^{Cre} and *Ripk1*$^{f/f}$*Foxp3*^{Cre} mice after stimulation with IL-2 (500 U/mL) or plate-bound anti-CD3/CD28 plus IL-2 for 48 h ($n = 4$). **D** Flow cytometry analysis of apoptotic and dead T_{reg} cells sorted from *Foxp3*^{Cre} and *Ripk1*$^{f/f}$*Foxp3*^{Cre} mice after stimulation with plate-bound anti-CD3/CD28 for 6 h using Annexin V and 7-AAD staining. **E** Volcano plot of RNA-seq data, with representative survival, activation/cytotoxic and T_{reg} signature genes shown. The horizontal dotted line indicates a p value of 0.05, and the vertical dotted lines indicate a fold change of 1.5. **F** Heatmap analysis of representative gene expression in *Foxp3*^{Cre} and *Ripk1*$^{f/f}$*Foxp3*^{Cre} T_{reg} cells. **G** Flow cytometry analysis of IFN-γ$^+$ or GzmB$^+$ T_{reg} cells in the spleen and LNs of 6-week-old *Foxp3*^{Cre} and *Ripk1*$^{f/f}$*Foxp3*^{Cre} mice. The left panel shows representative flow cytometry plots of IFN-γ$^+$ and GzmB$^+$ T_{reg} cells in the spleen and LNs. Numbers in quadrants indicate the percentage of cells in each respective quadrant. The right panel summarizes the percentages of IFN-γ$^+$ and GzmB$^+$ T_{reg} cells in the spleen or LNs ($n = 3$). Data in (**A**–**G**) are representative of at least two independent experiments. Data in (**C**) are mean ± s.e.m., ns not significant, $*p < 0.05$, and $***p < 0.001$ (two-tailed Student's t test)

related receptors. Interestingly, we also observed elevated expression levels of *Mlkl* and *Zbp1*, key molecules involved in the necroptosis pathway, in *Ripk1*$^{f/f}$*Foxp3*^{Cre} T_{reg} cells (Fig. 3E, F). This suggests that, in addition to apoptosis, RIPK1 may also participate in regulating necroptosis in T_{reg} cells.

Ablation of *Fadd* partially rescues RIPK1-deficient T_{reg} cells from cell death

RIPK1 participates in multiple signaling pathways, including FADD/Caspase8-dependent apoptosis and RIPK3/MLKL-dependent necroptosis. To investigate the involvement of the FADD/Caspase8 apoptotic pathway in the functions of RIPK1 in T_{reg} cells, we utilized *Ripk1*$^{f/f}$*Fadd*$^{-/-}$*Fadd:gfp*$^{f/f}$*CD4*^{Cre} mice to evaluate the elimination of *Fadd* in RIPK1-deficient T cells (Supplementary Fig. 5). Previous studies have reported that RIPK1 is essential for maintaining homeostasis in conventional T cells by inhibiting apoptosis [18]. Consistent with these findings, we observed a significant reduction in $CD4^+$ and $CD8^+$ T cells in *Ripk1*$^{f/f}$*CD4*^{Cre} mice. Under lymphopenic conditions, there was an increase in the proportion of activated $CD8^+$ T cells but not activated $CD4^+$ T cells in the lymph nodes of *Ripk1*$^{f/f}$*CD4*^{Cre} mice (Supplementary Fig. 6A). Despite the increase in activated $CD8^+$ T cells, there were no evident signs of autoimmune diseases in young *Ripk1*$^{f/f}$*CD4*^{Cre} mice (Supplementary Fig. 6B). This might be attributed to the overall reduction in effector T cells, particularly $CD4^+$ effector T cells, resulting from the deficiency of RIPK1. As expected, we observed that both $CD4^+$ and $CD8^+$ T cells in various organs of *Ripk1*$^{f/f}$*Fadd*$^{-/-}$*Fadd:gfp*$^{f/f}$*CD4*^{Cre} mice were restored to the levels in wild-type mice (Fig. 4A). Furthermore, we observed that the proportions of naive ($CD44^{low}CD62L^{high}$) and activated ($CD44^{high}CD62L^{low}$) T-cell subsets in *Ripk1*$^{f/f}$*Fadd*$^{-/-}$*Fadd:gfp*$^{f/f}$*CD4*^{Cre} mice were similar to those in wild-type $CD4^+$ and $CD8^+$ T cells, respectively (Supplementary Fig. 6A). These findings indicate that the RIPK1-FADD pathway is vital for maintaining the homeostasis of conventional T cells.

Surprisingly, unlike conventional T cells, T_{reg} cells were only partially restored in the spleens and lymph nodes in *Ripk1*$^{f/f}$*Fadd*$^{-/-}$*Fadd:gfp*$^{f/f}$*CD4*^{Cre} mice, although T_{reg} cells in the gut were rescued to wild-type levels (Fig. 4B). As the absence of RIPK1 and FADD in conventional T cells potentially impacts T_{reg} homeostasis in these mice, we conducted cotransfer experiments to confirm whether the reduction in T_{reg} cell number was intrinsic to T_{reg} cells themselves. We cotransferred T_{reg} cells from *Ripk1*$^{f/f}$*Fadd*$^{-/-}$*Fadd:gfp*$^{f/f}$*CD4*^{Cre} mice and $CD45.1^+$ wild-type T_{reg} cells into $CD45.1^+CD45.2^+$ wild-type recipient mice and analyzed their proportions in recipient mice on Day 7 and Day 14 after transfer. During these time points, we observed a gradual decrease in the proportion of T_{reg} cells from *Ripk1*$^{f/f}$*Fadd*$^{-/-}$*Fadd:gfp*$^{f/f}$*CD4*^{Cre} mice (Supplementary Fig. 6C), suggesting that T_{reg} cells deficient in RIPK1 and FADD do have inherent survival issues. Notably, despite only partial restoration of T_{reg} cells in *Ripk1*$^{f/f}$*Fadd*$^{-/-}$*Fadd:gfp*$^{f/f}$*CD4*^{Cre} mice, the extent of T_{reg} cell restoration was sufficient to prevent autoimmune diseases (Supplementary Fig. 6B). Taken together, our findings demonstrate the critical role of the RIPK1-FADD pathway in maintaining T_{reg} cell homeostasis and function, with other RIPK1-mediated pathways also being involved.

Pro-apoptotic BH3-only proteins have previously been reported to play a role in the regulation of T_{reg} cell apoptosis [3]. Therefore, we proceeded to investigate whether Bim, one such protein, contributes to the cell death observed in RIPK1-deficient T_{reg} cells using *Bcl2l11*$^{-/-}$*Ripk1*$^{f/f}$*Foxp3*^{Cre} mice. We found that Bim ablation did not facilitate the restoration of the T_{reg} population (Supplementary Fig. 7), which suggests that Bim may not be directly involved in the cell death of RIPK1-deficient T_{reg} cells.

We subsequently investigated whether blocking RIPK3/MLKL can facilitate the restoration of the T_{reg} population by utilizing *Ripk3*$^{-/-}$*Ripk1*$^{f/f}$*Foxp3*^{Cre} mice, which have both *Ripk3* and *Ripk1* deletion in T_{reg} cells. Compared to *Ripk1*$^{f/f}$*Foxp3*^{Cre} mice, *Ripk3*$^{-/-}$*Ripk1*$^{f/f}$*Foxp3*^{Cre} mice displayed a significant reduction in the percentages of T_{reg} cells in the spleen and lymph nodes (Supplementary Fig. 8A). As anticipated, *Ripk3*$^{-/-}$*Ripk1*$^{f/f}$*Foxp3*^{Cre} mice showed severe inflammatory symptoms characterized by the activation of conventional $CD4^+$ T cells and $CD8^+$ T cells, as well as lymphocyte infiltration in various organs (Supplementary Fig. 8B, C). These findings suggest that solely blocking necroptosis is insufficient to rescue T_{reg} cells from the death caused by RIPK1 deficiency.

Deletion of *Fadd* and *Ripk3* completely rescues cell death in RIPK1-deficient T_{reg} cells

Since blocking either the *Fadd* pathway or the *Ripk3* pathway alone cannot fully rescue T_{reg} cells from the death caused by RIPK1 deficiency, we hypothesized that RIPK1 deficiency may lead to both necroptosis and apoptosis in T_{reg} cells. To investigate this hypothesis, we utilized *Ripk3*$^{-/-}$*Ripk1*$^{-/-}$*Fadd*$^{-/-}$ mice, which lack both FADD-mediated apoptosis and RIPK3-mediated necroptosis [12]. As expected, these mice exhibited normal conventional $CD4^+$ and $CD8^+$ T compartments (Fig. 5A), similar to *Ripk1* and *Fadd* double knockout mice. However, unlike *Ripk1* and *Fadd* double knockout mice, *Ripk3*$^{-/-}$*Ripk1*$^{-/-}$*Fadd*$^{-/-}$ mice showed normal percentages of T_{reg} cells in all examined organs, including the thymus, spleen, lymph nodes, small intestine and colon (Fig. 5B). Additionally, we observed that T_{reg} cells from *Ripk3*$^{-/-}$*Ripk1*$^{-/-}$*Fadd*$^{-/-}$ mice recovered from cell death under in vitro TCR stimulation (Supplementary Fig. 9A) and exhibited normal suppressive function in vitro compared to wild-type T_{reg} cells (Supplementary Fig. 9B). Moreover, no autoimmune diseases were detected in these mice (Supplementary Fig. 9C, D). These findings strongly suggest that the removal of *Fadd* and *Ripk3* greatly improved the cell survival and functions of RIPK1-deficient T_{reg} cells. Since triple knockout mice are not conditional knockout mice, we further analyzed T_{reg} cells in chimeric mice reconstituted with *Ripk3*$^{-/-}$*Ripk1*$^{-/-}$*Fadd*$^{-/-}$ bone marrow to validate our observations in a more controlled model. Compared to wild-type bone marrow chimeras, *Ripk3*$^{-/-}$*Ripk1*$^{-/-}$*Fadd*$^{-/-}$ bone marrow chimeras also exhibited normal T_{reg} cell percentages and numbers (Supplementary Fig. 10). Together, these results demonstrate that RIPK1 functions to inhibit both FADD-mediated apoptosis and RIPK3-mediated necroptosis in T_{reg} cells.

DISCUSSION

T-cell homeostasis, achieved by a well-orchestrated balance of T-cell survival and death, is crucial for a functional immune system. Receptor-interacting protein kinase 1 (RIPK1) has been identified as a master regulator of apoptosis, necroptosis and inflammation, depending on cell type and context [14, 21–23]. Although RIPK1 is not essential for T-cell development in the thymus, it is crucial for conventional T-cell homeostasis because it inhibits apoptosis [18]. In our study, we observed an increase in the percentage of CD4SP thymocytes in 6-week-old *Ripk1*$^{f/f}$*Foxp3*^{Cre} mice compared to WT mice (Fig. 5A), which is likely due to a secondary effect of the severe autoimmune diseases present in *Ripk1*$^{f/f}$*Foxp3*^{Cre} mice. As a special subset of $CD4^+$ T cells, T_{reg} cells have quite different homeostasis mechanisms from conventional $CD4^+$ T cells. It remains unclear whether RIPK1 has similar functions in T_{reg} cell homeostasis. In this study, we found that T_{reg} cell-specific ablation of *Ripk1* leads to fatal systemic autoimmunity due to excessive T_{reg} cell death. Unlike conventional T cells, T_{reg} cells with RIPK1 deficiency are only partially rescued by *Fadd* deletion. However, the deletion of both *Fadd* and *Ripk3* completely rescued T_{reg} cells from death in *Ripk1*-deficient mice. Our results demonstrate that RIPK1 regulates T_{reg} cell survival by controlling both necroptosis and apoptosis.

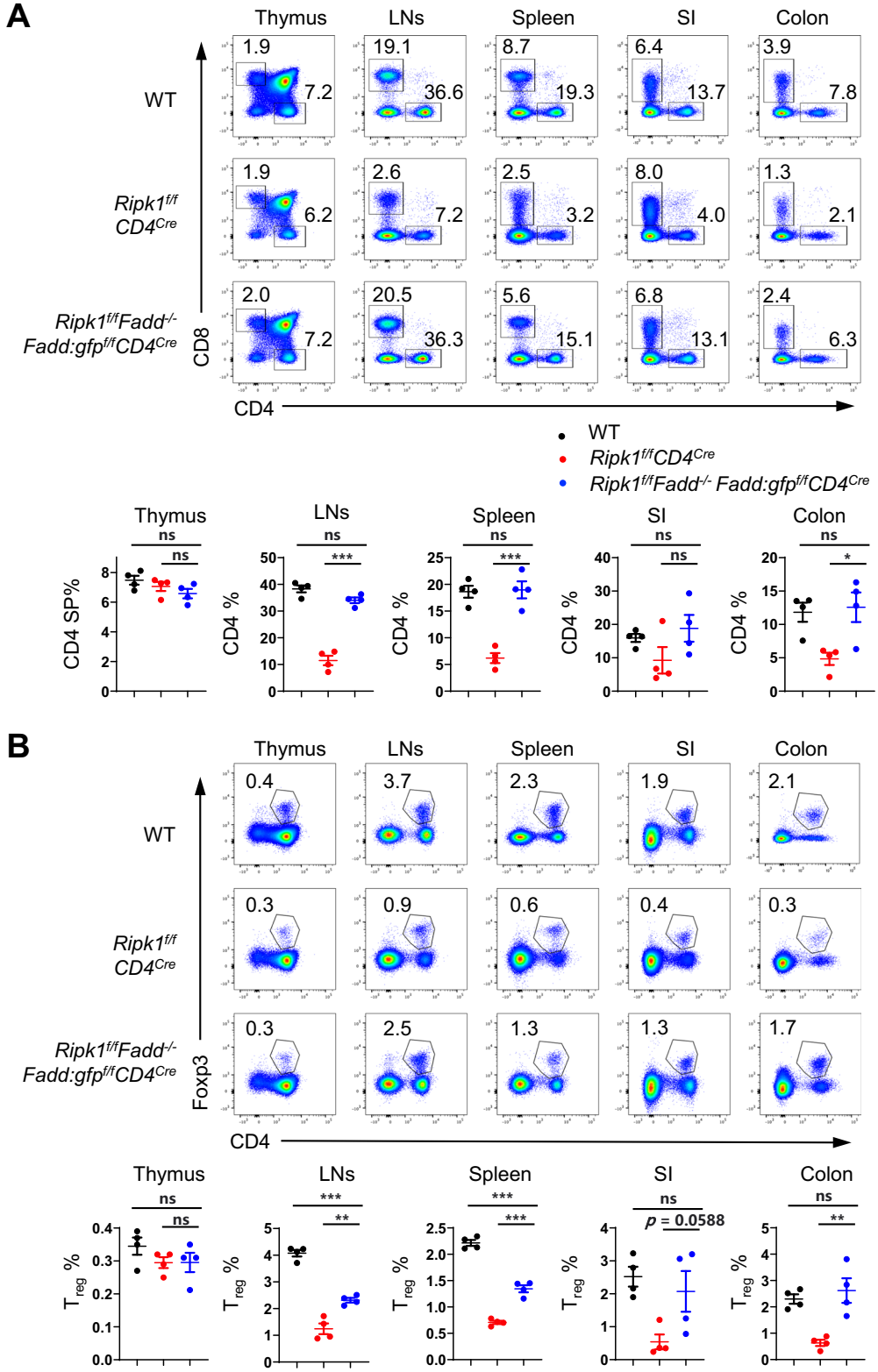

Fig. 4 Ablation of *Fadd* partially rescues RIPK1-deficient T_{reg} cells from cell death. **A** Flow cytometry analysis of CD4SP and CD8SP thymocytes in the thymus and $CD4^+$ and $CD8^+$ T cells in the lymph nodes (LNs), spleen, small intestine (SI), and colon from 6-week-old WT, *Ripk1*$^{f/f}$*CD4*^{Cre} and *Ripk1*$^{f/f}$*Fadd*$^{-/-}$*Fadd:gfp*$^{f/f}$*CD4*^{Cre} mice (upper panel); numbers adjacent to the outlined areas indicate the percentages of CD4SP and CD8SP in the thymus and $CD4^+$ T and $CD8^+$ T cells in the LNs, spleen, SI, and colon. The percentages of CD4SP or $CD4^+$ T cells are summarized ($n = 4$, lower panel). **B** Flow cytometry analysis of $Foxp3^+$ T_{reg} cells in the thymus, LNs, spleen, SI and colon from 6-week-old WT, *Ripk1*$^{f/f}$*CD4*^{Cre} and *Ripk1*$^{f/f}$*Fadd*$^{-/-}$*Fadd:gfp*$^{f/f}$*CD4*^{Cre} mice (upper panel). Numbers adjacent to the outlined areas indicate the percentages of $Foxp3^+$ T_{reg} cells in the thymus, LNs, spleen, SI and colon. The percentages of $Foxp3^+$ T_{reg} cells are summarized ($n = 4$, lower panel). Data in (**A**, **B**) are representative of at least two independent experiments. Data in (**A:** lower panel, **B:** lower panel) are mean ± s.e.m., ns, not significant, $^*p < 0.05$, $^{**}p < 0.01$, $^{***}p < 0.001$ (two-tailed Student's *t* test)

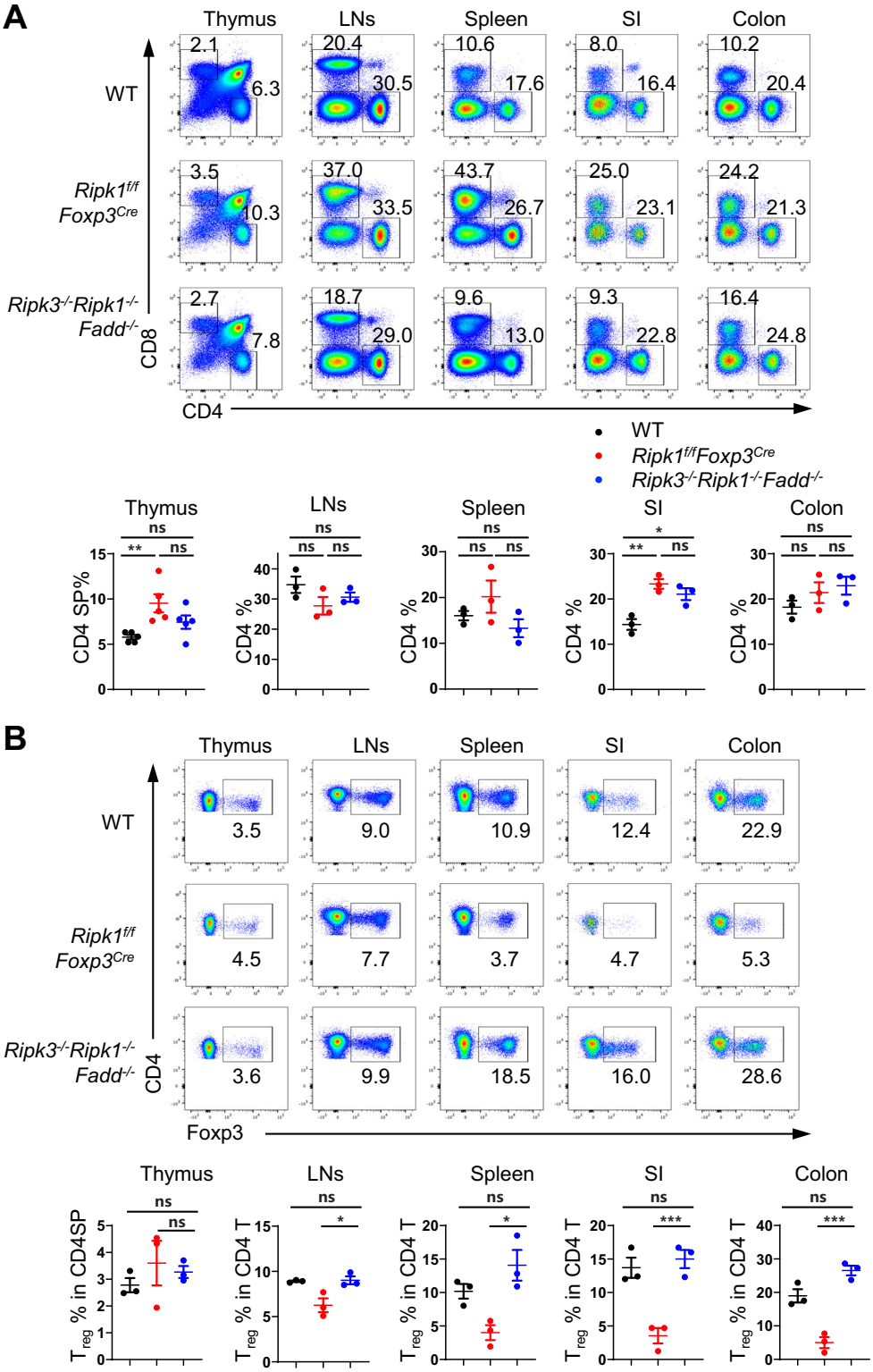

Fig. 5 Deletion of *Fadd* and *Ripk3* completely rescues cell death in RIPK1-deficient T_{reg} cells. **A** Flow cytometry analysis of CD4SP and CD8SP thymocytes in the thymus and $CD4^+$ and $CD8^+$ T cells in the lymph nodes (LNs), spleen, small intestine (SI), and colon from 6-week-old WT, *Ripk1*$^{f/f}$*Foxp3*^{Cre} and *Ripk3*$^{-/-}$*Ripk1*$^{-/-}$*Fadd*$^{-/-}$ mice (upper panel); numbers adjacent to the outlined areas indicate the percentages of CD4SP and CD8SP in the thymus and $CD4^+$ T and $CD8^+$ T cells in the LNs, spleen, SI, and colon. The percentages of CD4SP or $CD4^+$ T cells are summarized in the lower panel ($n = 5$ in thymus; $n = 3$ in LNs, spleen, SI, colon). **B** Flow cytometry analysis of $Foxp3^+$ T_{reg} cells in CD4SP cells in the thymus and $CD4^+$ T cells in the LNs, spleen, SI and colon from 6-week-old WT, *Ripk1*$^{f/f}$*Foxp3*^{Cre} and *Ripk3*$^{-/-}$*Ripk1*$^{-/-}$*Fadd*$^{-/-}$ mice (upper panel). Numbers adjacent to the outlined areas indicate the percentages of $Foxp3^+$ T_{reg} cells in CD4SP in the thymus and $CD4^+$ T cells in the LNs, spleen, SI and colon. The percentages of $Foxp3^+$ T_{reg} cells are summarized ($n = 3$, lower panel). Data in (**A**, **B**) are representative of at least two independent experiments. Data in (**A:** lower panel, **B:** lower panel) are mean ± s.e.m., ns not significant, $*p < 0.05$, $**p < 0.01$, and $***p < 0.001$ (two-tailed Student's *t* test)

Mature T cells, including T_{reg} cells, rely on TCR signaling to maintain their homeostasis. However, the mechanisms by which TCR regulates T-cell homeostasis remain to be elucidated. Our study reveals that TCR stimulation can induce the upregulation of RIPK1, which plays a vital role in T_{reg} cell survival upon TCR stimulation. This indicates that RIPK1 function is essential for TCR-mediated T-cell homeostasis. Although there is currently no direct evidence implicating RIPK1 in TCR signal transduction, it has been demonstrated that MALT1, downstream of TCR signals, regulates the activation of caspase-8, which can form a complex with RIPK1 and c-FLIPs [24, 25]. Therefore, it is plausible that RIPK1 promotes T_{reg} cell survival through its interaction with MALT1 and caspase-8, which warrants further investigation.

The RIPK1 protein comprises a kinase domain in its N-terminus, an RHIM domain, and a death domain in its C-terminus, each with distinct functional sites where posttranslational modifications such as ubiquitination and phosphorylation can occur [26]. Recent studies have demonstrated the critical role of RIPK1 ubiquitination at K376 in both apoptosis and necroptosis in vitro and in vivo [27–29]. However, in *Ripk1*$^{f/K376R}$*CD4*^{Cre} mice, we did not observe any abnormalities in T_{reg} cell development or homeostasis (Supplementary Fig. 11). This suggests that while RIPK1 ubiquitination on the K376-mediated pathway is essential for suppressing cell death during embryogenesis and postnatal inflammation, it is not required for T_{reg} cell homeostasis. Additionally, research has shown that phosphorylated RIPK1 can translocate to the nucleus, where it regulates chromatin remodeling and transcriptional control of inflammatory factors [30]. Therefore, in T_{reg} cell homeostasis and during T_{reg} activation, RIPK1 may serve not only as a vital protein for cell survival but also as a regulator of relevant gene expression. Our study revealed alterations in the expression levels of multiple genes in response to RIPK1 deficiency. Further investigation is necessary to determine whether these genes are directly regulated by phosphorylated RIPK1.

T_{reg} cells are not a homogenous population but instead display some degree of heterogeneity in their phenotypes, functions, and lineage origins [4]. Our study has revealed intriguing insights into the differential roles played by RIPK1 in various subpopulations of T_{reg} cells. Specifically, we found that RIPK1 deficiency leads to greater loss of activated T_{reg} (aT_{reg}) cells, suggesting that aT_{reg} cells rely more on RIPK1 to maintain homeostasis than resting T_{reg} (rT_{reg}) cells. Within the gut mucosa, T_{reg} cells include a significant proportion of peripherally induced T_{reg} (pT_{reg}) cells that are derived from conventional $CD4^+$ T cells [31, 32]. Strikingly, our research demonstrated that under steady-state conditions, RIPK1-deficient T_{reg} cells in the gut can be fully rescued through the deletion of the *Fadd* gene, whereas the same restorative effect is not observed in their counterparts within secondary lymphoid organs. These findings imply that while RIPK1 may have similar functions in pT_{reg} cells and conventional $CD4^+$ T cells, it exerts distinct effects on thymus-derived T_{reg} (tT_{reg}) cells.

Studies have provided evidence that the responsiveness of tumor-infiltrating T_{reg} cells to microenvironmental signals can disrupt their stability and survival, thereby influencing the outcome of antitumor immune responses [33]. Our findings suggest that under steady-state conditions, the primary function of RIPK1 is to suppress T_{reg} cell death and maintain self-tolerance. However, it remains to be determined whether manipulating RIPK1 expression in T_{reg} cells within the tumor microenvironment or other pathological contexts could be leveraged as a strategic approach to modulate disease progression. Further investigations are warranted to shed light on this important aspect.

In summary, our study highlights the critical role of RIPK1 in preserving T_{reg} cell homeostasis by restraining both RIPK3- and FADD-mediated cell death pathways. These findings provide fresh insights into the underlying mechanisms that govern the balance and stability of T_{reg} cells.

MATERIALS AND METHODS

Mice

The *Ripk1*$^{f/f}$ mice were generated by a homologous recombination strategy (Shanghai Model Organisms Center, Inc.). In brief, hybrid mouse embryonic stem (ES) cells were electroporated with a targeting vector containing floxed *exon 3*. The *Ripk3*$^{-/-}$ mice were provided by Dr. Xiaodong Wang (National Institute of Biological Sciences, Beijing, China), and the *Fadd*$^{-/-}$*Fadd:gfp*$^{f/f}$ mice were provided by Dr. Jianke Zhang (Thomas Jefferson University, Philadelphia, PA, USA), as previously described [34]. *CD4*^{Cre} and *Foxp3*$^{YFP\text{-}Cre}$ (*Foxp3*^{Cre}) mice were provided by Dr. Bin Li (Shanghai Institute of Immunology, Shanghai Jiao Tong University, Shanghai, China). *Ripk1*$^{f/f}$*CD4*^{Cre} and *Ripk1*$^{f/f}$*Foxp3*^{Cre} mice were generated by crossing *Ripk1*$^{f/f}$ mice with *CD4*^{cre} or *Foxp3*^{Cre} mice, respectively. *Ripk1*$^{f/f}$*Fadd*$^{-/-}$*Fadd:gfp*$^{f/f}$*CD4*^{Cre} mice were obtained by breeding *Fadd*$^{-/-}$*Fadd:gfp*$^{f/f}$ mice with *Ripk1*$^{f/f}$*CD4*^{Cre} mice. The $CD45.1^+$ mice were provided by Dr. Qibin Leng (Institut Pasteur of Shanghai). All mice were maintained under specific pathogen-free conditions at the Institut Pasteur of Shanghai or Tongji University in China. All animal experiments were performed following the protocols approved by the Institutional Animal Care and Use Committee of the Institut Pasteur of Shanghai or Shanghai East Hospital, Tongji University.

Flow cytometry and cell sorting

For surface marker staining, cells were washed with staining buffer (PBS containing 1% FBS and 1 mM EDTA). To block nonspecific binding, anti-CD16/CD32 antibodies (2.4G2) were added, followed by a 30-minute incubation with surface antibodies on ice. The antibodies used for FACS analysis included APC-Cy7-anti-CD4 (GK1.5, Thermo Fisher Scientific), PE-Cy7-anti-CD4 (GK1.5, Thermo Fisher Scientific), PE-Cy7-anti-CD8 (53–6.7, Thermo Fisher Scientific), PerCP-Cy5.5-anti-CD8 (53–6.7, BioLegend), PE-anti-CD44 (IM7, Thermo Fisher Scientific), APC-anti-CD62L (MEL-14, Thermo Fisher Scientific), PE-Cy7-anti-CD25 (PC61.5, Thermo Fisher Scientific), PE-anti-TNFR1 (55R-286, BioLegend), PE-Cy7-anti-PD-1 (29 F.1A12, BioLegend), and AF647-anti-FAS (Jo2, BD Bioscience). Dead cells were excluded using a Live/Dead Fixable Aqua Dead Cell staining kit (Thermo Fisher Scientific). Samples were acquired using an LSRFortessa flow cytometer (BD PharMingen) and analyzed by FlowJo software (TreeStar).

For cytokine staining, cells were stimulated with 10 ng/mL PMA (phorbol 12-myristate 13-acetate, Sigma, St. Louis, MO) and 1 μg/mL ionomycin (Sigma) for 4 h. After treatment with 10 μg/mL brefeldin A (Sigma) for another 2 h, surface markers were stained, and cells were fixed with 3.7% formaldehyde for 15 min at room temperature. Subsequently, the cells were permeabilized with 0.2% saponin in PBS on ice for 20 min before intracellular staining. Samples were acquired using an LSRFortessa flow cytometer (BD PharMingen) and analyzed by FlowJo software (TreeStar).

To sort T_{conv} and T_{reg} cells, $CD4^+$ T cells were enriched by negative selection using biotin-labeled CD8a, TER-119 and B220 antibodies and streptavidin magnetic beads (Magnet sort, Thermo). $CD44^{low}CD62L^{high}$ naive $CD4^+$ T cells or $CD4^+YFP^+$ T_{reg} cells were sorted by a FACS Aria II cell sorter (BD Bioscience). The sorted cell populations were >98% pure.

Isolation of tissue-resident lymphocytes

To isolate lamina propria (LP) mononuclear cells, small intestines and colons were dissected, and fat tissues and Peyer's patches were removed. Predigestion was performed using PBS containing 1 mM DTT (Sigma) and 30 mM EDTA (AMResco) at 37 °C for 30 min. Then, the pretreated tissues were digested with Liberase (250 μg/mL, Roche) and DNase I (200 μg/mL, Sigma) in DMEM supplemented with 5% FBS at 37 °C for 30 min in a shaker. The digested tissues were then meshed in a 70 μm cell strainer and subjected to Percoll gradient (40%/80%) centrifugation. Mononuclear cells present in the interphase were collected, washed with PBS and resuspended in T-cell medium.

Construction of bone marrow chimeras

To generate bone marrow chimeras, bone marrow cells from either wild-type or *Ripk3*$^{-/-}$*Ripk1*$^{-/-}$*Fadd*$^{-/-}$ mice were transferred to 6- to 8-week-old *TCRβ*$^{-/-}$ recipient mice that had been irradiated with 450 rads. After 2 weeks of neomycin treatment, the chimeric mice were analyzed following a 6-week reconstitution period.

T_{reg} cell cotransference

T_{reg} cells were isolated from the spleens and lymph nodes of *Ripk1*$^{f/f}$*Fadd*$^{-/-}$*Fadd:gfp*$^{f/f}$*CD4*^{Cre} mice or $CD45.1^+$ wild-type mice using a T_{reg} cell

isolation kit (Miltenyi Biotec). T_{reg} cells from *Ripk1*$^{f/f}$*Fadd*$^{-/-}$*Fadd:gfp*$^{f/f}$*CD4*^{Cre} mice were then mixed with CD45.1$^+$ wild-type cells at a 1:1 ratio and subsequently transferred into CD45.1$^+$CD45.2$^+$ wild-type recipient mice via intravenous injection. The proportions of transferred T_{reg} cells in the recipient mice were analyzed 1 and 2 weeks after transfer.

In vitro T_{reg} suppression assay

The in vitro T_{reg} suppression assay was performed as previously described [35]. Briefly, CD4$^+$CD25$^-$CD45RB^{high} naive CD4$^+$ T cells and CD4$^+$CD25$^+$CD45RB^{low} T_{reg} cells were sorted using fluorescence-activated cell sorting (FACS). Naive CD4$^+$ T cells were labeled with CellTrace Violet (Thermo Fisher Scientific) and cocultured with T_{reg} cells at a 1:1 ratio on a plate coated with anti-CD3/anti-CD28 antibodies for 72 h. Subsequently, the dilution of CellTrace was analyzed using flow cytometry.

Cell viability assay

Cell viability was measured using the CellTiter-Glo Luminescent Cell Viability Assay kit (Promega) according to the manufacturer's instructions. The luminescence was recorded with a microplate luminometer (Thermo Scientific).

Histopathology

For histological analysis, the samples were fixed in 3.7% formaldehyde, dehydrated in ethanol, cleared with xylene, and embedded in paraffin. Thin sections, approximately five micrometers thick, were cut and mounted onto glass slides that had been precoated with poly-l-lysine. These sections were then stained with hematoxylin and eosin using standard procedures.

RNA-Seq analysis

Total RNA was extracted using TRIzol reagent (Life Technologies) following the manufacturer's instructions. The quality of the RNA was evaluated, and sequencing was performed using the Illumina HiSeq X platform at Novogene (Beijing, China). Raw data from the sequencer underwent preprocessing, alignment, and deduplication before being exported as raw counts. The differential expression gene analysis was conducted using the R package DESeq2 [36]. For the generation of the heatmap, the raw counts were transformed using the variance stabilizing transformation method and used as input. The RNA-seq data have been deposited in the Gene Expression Omnibus under the primary accession code GSE230483.

Statistical analysis

Statistical analysis were performed using Prism 9 (GraphPad). Two-tailed Student's *t* tests and paired *t* tests were used to calculate *p* values ($^*p < 0.05$, $^{**}p < 0.01$ and $^{***}p < 0.001$). The data presented in this article are the representative results of at least two independent experiments.

REFERENCES

1. Sakaguchi S, Mikami N, Wing JB, Tanaka A, Ichiyama K, Ohkura N. Regulatory T cells and human disease. Annu Rev Immunol. 2020;38:541–66.
2. Smigiel KS, Srivastava S, Stolley JM, Campbell DJ. Regulatory T-cell homeostasis: steady-state maintenance and modulation during inflammation. Immunol Rev. 2014;259:40–59.
3. Pierson W, Cauwe B, Policheni A, Schlenner SM, Franckaert D, Berges J, et al. Antiapoptotic Mcl-1 is critical for the survival and niche-filling capacity of Foxp3$^+$ regulatory T cells. Nat Immunol. 2013;14:959–65.
4. Liston A, Gray DHD. Homeostatic control of regulatory T cell diversity. Nat Rev Immunol. 2014;14:154–65.
5. Levine AG, Arvey A, Jin W, Rudensky AY. Continuous requirement for the TCR in regulatory T cell function. Nat Immunol. 2014;15:1070–8.
6. Huehn J, Siegmund K, Lehmann JC, Siewert C, Haubold U, Feuerer M, et al. Developmental stage, phenotype, and migration distinguish naive- and effector/memory-like CD4+ regulatory T cells. J Exp Med. 2004;199:303–13.
7. Wang CY, Mayo MW, Korneluk RG, Goeddel DV, Baldwin AS Jr. NF-kappaB anti-apoptosis: induction of TRAF1 and TRAF2 and c-IAP1 and c-IAP2 to suppress caspase-8 activation. Science. 1998;281:1680–3.
8. Petersen SL, Wang L, Yalcin-Chin A, Li L, Peyton M, Minna J, et al. Autocrine TNFalpha signaling renders human cancer cells susceptible to Smac-mimetic-induced apoptosis. Cancer Cell. 2007;12:445–56.
9. Wang L, Du F, Wang X. TNF-alpha induces two distinct caspase-8 activation pathways. Cell. 2008;133:693–703.
10. Sun L, Wang H, Wang Z, He S, Chen S, Liao D, et al. Mixed lineage kinase domain-like protein mediates necrosis signaling downstream of RIP3 kinase. Cell. 2012;148:213–27.
11. Zhao J, Jitkaew S, Cai Z, Choksi S, Li Q, Luo J, et al. Mixed lineage kinase domain-like is a key receptor interacting protein 3 downstream component of TNF-induced necrosis. Proc Natl Acad Sci USA. 2012;109:5322–7.
12. Dillon CP, Weinlich R, Rodriguez DA, Cripps JG, Quarato G, Gurung P, et al. RIPK1 blocks early postnatal lethality mediated by caspase-8 and RIPK3. Cell. 2014;157:1189–202.
13. Kearney CJ, Cullen SP, Clancy D, Martin SJ. RIPK1 can function as an inhibitor rather than an initiator of RIPK3-dependent necroptosis. FEBS J. 2014;281:4921–34.
14. Dannappel M, Vlantis K, Kumari S, Polykratis A, Kim C, Wachsmuth L, et al. RIPK1 maintains epithelial homeostasis by inhibiting apoptosis and necroptosis. Nature. 2014;513:90–4.
15. Tan S, Zhao J, Sun Z, Cao S, Niu K, Zhong Y, et al. Hepatocyte-specific TAK1 deficiency drives RIPK1 kinase-dependent inflammation to promote liver fibrosis and hepatocellular carcinoma. Proc Natl Acad Sci USA. 2020;117:14231–42.
16. Cuchet-Lourenco D, Eletto D, Wu C, Plagnol V, Papapietro O, Curtis J, et al. Biallelic RIPK1 mutations in humans cause severe immunodeficiency, arthritis, and intestinal inflammation. Science. 2018;361:810–3.
17. Li Y, Fuhrer M, Bahrami E, Socha P, Klaudel-Dreszler M, Bouzidi A, et al. Human RIPK1 deficiency causes combined immunodeficiency and inflammatory bowel diseases. Proc Natl Acad Sci USA. 2019;116:970–5.
18. Dowling JP, Cai Y, Bertin J, Gough PJ, Zhang J. Kinase-independent function of RIP1, critical for mature T-cell survival and proliferation. Cell Death Dis. 2016;7:e2379.
19. Smigiel KS, Richards E, Srivastava S, Thomas KR, Dudda JC, Klonowski KD, et al. CCR7 provides localized access to IL-2 and defines homeostatically distinct regulatory T cell subsets. J Exp Med. 2014;211:121–36.
20. Luo CT, Liao W, Dadi S, Toure A, Li MO. Graded Foxo1 activity in Treg cells differentiates tumour immunity from spontaneous autoimmunity. Nature. 2016;529:532–6.
21. Takahashi N, Vereecke L, Bertrand MJ, Duprez L, Berger SB, Divert T, et al. RIPK1 ensures intestinal homeostasis by protecting the epithelium against apoptosis. Nature. 2014;513:95–9.
22. Roderick JE, Hermance N, Zelic M, Simmons MJ, Polykratis A, Pasparakis M, et al. Hematopoietic RIPK1 deficiency results in bone marrow failure caused by apoptosis and RIPK3-mediated necroptosis. Proc Natl Acad Sci USA. 2014;111:14436–41.
23. Mifflin L, Ofengeim D, Yuan J. Receptor-interacting protein kinase 1 (RIPK1) as a therapeutic target. Nat Rev Drug Discov. 2020;19:553–71.
24. Su H, Bidere N, Zheng L, Cubre A, Sakai K, Dale J, et al. Requirement for caspase-8 in NF-kappaB activation by antigen receptor. Science. 2005;307:1465–8.
25. Misra RS, Russell JQ, Koenig A, Hinshaw-Makepeace JA, Wen R, Wang D, et al. Caspase-8 and c-FLIPL associate in lipid rafts with NF-kappaB adaptors during T cell activation. J Biol Chem. 2007;282:19365–74.
26. Shan B, Pan H, Najafov A, Yuan J. Necroptosis in development and diseases. Genes Dev. 2018;32:327–40.
27. Zhang X, Zhang H, Xu C, Li X, Li M, Wu X, et al. Ubiquitination of RIPK1 suppresses programmed cell death by regulating RIPK1 kinase activation during embryogenesis. Nat Commun. 2019;10:4158.
28. Tang Y, Tu H, Zhang J, Zhao X, Wang Y, Qin J, et al. K63-linked ubiquitination regulates RIPK1 kinase activity to prevent cell death during embryogenesis and inflammation. Nat Commun. 2019;10:4157.
29. Kist M, Kőműves LG, Goncharov T, Dugger DL, Yu C, Roose-Girma M, et al. Impaired RIPK1 ubiquitination sensitizes mice to TNF toxicity and inflammatory cell death. Cell Death Differ. 2021;28:985–1000.
30. Li W, Shan B, Zou C, Wang H, Zhang MM, Zhu H, et al. Nuclear RIPK1 promotes chromatin remodeling to mediate inflammatory response. Cell Res. 2022;32:621–37.
31. Bilate AM, Lafaille JJ. Induced CD4+Foxp3+ regulatory T cells in immune tolerance. Annu Rev Immunol. 2012;30:733–58.
32. Lathrop SK, Bloom SM, Rao SM, Nutsch K, Lio CW, Santacruz N, et al. Peripheral education of the immune system by colonic commensal microbiota. Nature. 2011;478:250–4.
33. Barbi J, Pardoll D, Pan F. Treg functional stability and its responsiveness to the microenvironment. Immunol Rev. 2014;259:115–39.
34. Zhang Y, Rosenberg S, Wang H, Imtiyaz HZ, Hou YJ, Zhang J. Conditional Fas-associated death domain protein (FADD): GFP knockout mice reveal FADD is dispensable in thymic development but essential in peripheral T cell homeostasis. J Immunol. 2005;175:3033–44.

35. Collison LW, Vignali DA. In vitro Treg suppression assays. Methods Mol Biol. 2011;707:21–37.
36. Love MI, Huber W, Anders S. Moderated estimation of fold change and dispersion for RNA-seq data with DESeq2. Genome Biol. 2014;15:550.

ACKNOWLEDGEMENTS

This work was supported by the following grants: National Key Research and Development Program of China (2021YFA1301402), Shanghai Municipal Science and Technology Major Project (ZD2021CY001), National Key Research and Development Program of China (2021YFE0200900; 2022YFA0807300), National Natural Science Foundation of China (82101833, 82073901), Three-year Action Plan for Shanghai TCM Development and Inheritance Program [ZY(2021-2023)-0103], Top-level Clinical Discipline Project of Shanghai Pudong District (grant/award number: PWYgf 2021-01), and Training Plan for Discipline Leaders of Shanghai Pudong New Area Health Commission (grant/award number: PWRd2020-09).

AUTHOR CONTRIBUTIONS

HZ and HW conceived and supervised the research; XD, LW, YZ, ZY, YC, YS, YZ, HZ and HW contributed to the project design and discussions; XD, LW and YZ conducted the experiments; QL, YZ, WZ, YT, TW and JD helped with the mixed bone marrow chimera experiments and some phenotype analysis; FD and JR assisted with mouse models; PH did the bioinformatics analysis; XD, LW, YZ, ZY, YZ, HZ and HW wrote and edited the manuscript.

COMPETING INTERESTS

The authors declare no competing interests.

ADDITIONAL INFORMATION

Supplementary information The online version contains supplementary material available at https://doi.org/10.1038/s41423-023-01113-x.

Correspondence and requests for materials should be addressed to Yuejuan Zheng, Haibing Zhang or Haikun Wang.